High-Pressure Studies of CO Adsorption on Pd(111) by X-ray Photoelectron Spectroscopy and Sum-Frequency Generation

Vasiliy V. Kaichev, Igor P. Prosvirin, and Valerii I. Bukhtiyarov

Boreskov Institute of Catalysis of SB RAS, Lavrentieva ave. 5, Novosibirsk 630090, Russia

Holger Unterhalt, Günther Rupprechter,* and Hans-Joachim Freund

Fritz-Haber-Institut der Max-Planck-Gesellschaft, Faradayweg 4−6, D-14195 Berlin, Germany

Received: September 6, 2002

High-pressure CO adsorption on Pd(111) was examined by X-ray photoelectron spectroscopy (XPS) and vibrational sum frequency generation (SFG) from 200 to 400 K, and in a pressure range from 10^{-6} to 1 mbar. Even in the millibar regime both methods indicated that CO adsorbed in "regular" adsorption sites such as hollow, bridge, and on-top. By combination of XPS and SFG, a quantitative analysis of CO coverages at various pressures was performed. At high pressure, no CO structures different from those known from UHV studies were observed. Also, no indications of CO dissociation or carbonyl formation were found under the given experimental conditions, provided that the CO gas was sufficiently cleaned.

Introduction

The adsorption of carbon monoxide on palladium has attracted much attention, in part due to its practical relevance in heterogeneous catalysis for CO abatement from car exhausts. Furthermore, CO was often used as a probe molecule to characterize binding sites because the understanding of the structure of molecular overlayers on metal surfaces is essential for many processes. The CO/Pd(111) system has been extensively studied in the past by various surface-sensitive techniques such as temperature-programmed desorption (TPD),[1,2] low-energy electron diffraction (LEED),[3−8] X-ray photoelectron diffraction (XPD),[9] infrared reflection absorption spectroscopy (IRAS),[6,7,10−13] X-ray photoelectron spectroscopy (XPS),[14] scanning tunneling microscopy (STM),[15,16] and others.

It has been shown that CO forms a large number of ordered structures on Pd(111) and although there is still some debate on the exact structure of some (especially in the coverage range around 0.5 monolayer; see below), the understanding of CO adsorption on Pd(111) seems rather complete. One may assume that this knowledge may be successfully transferred to heterogeneous catalytic reactions. However, the results mentioned above have mostly been obtained in ultrahigh vacuum (UHV) or at low pressure (below 10^{-4} mbar) and one cannot take for granted that UHV results can be simply extrapolated to high-pressure reactions.[17−20] High pressures may lead to surface coverages or structures of adsorbates that cannot be obtained under typical UHV conditions. High pressures may also produce weakly bonded species, which are absent under UHV. In addition, surface compositions under UHV may differ substantially from the real catalyst conditions[21,22] and processes that are simply too slow under UHV may become significant at high pressure.

These questions can be addressed by surface-sensitive techniques that are able to operate in a high-pressure (mbar) regime, such as vibrational sum frequency generation (SFG) spectroscopy.[17,23] As a second-order nonlinear optical process, infrared-visible SFG is forbidden in media with inversion symmetry under the electric dipole approximation but allowed at the surface/interface where the inversion symmetry is broken. Consequently, SFG specifically probes the interfacial region between the isotropic gas phase and the centrosymmetric metallic bulk, and the SFG signal is dominated by adsorbed species.

Some of us have recently reported SFG spectra of CO adsorbed on Pd(111) from UHV to 1 bar.[19,24] The high-pressure structures were shown to be very similar to high-coverage structures under UHV. One question that could not be answered in refs 19 and 24 concerned the possibility of CO dissociation under high pressure. Although CO does not dissociate on single-crystal Pd surfaces in UHV,[3,25−28] the situation may change at high pressure. In a number of investigations on Pt,[29,30] it was reported that at high pressure CO dissociated and/or formed carbonyls even on the closed-packed Pt(111) surface by the Boudouard reaction $2CO \rightarrow C + CO_2$, leading to carbon deposition. Partial CO dissociation was also observed on Pd nanoparticles supported on various supports.[28,31−36] In this respect, carbon deposition is an undesired effect leading to catalyst deactivation.

It is clear that the detection of carbon residue from CO dissociation requires a method that unambiguously reveals the chemical composition of adlayers. Core-level photoelectron spectroscopy is the apparent method of choice. Although there are not many systematic studies of the CO/Pd(111) system using X-ray photoelectron spectroscopy, it is well-known that XPS allows us to distinguish molecular CO (C1s binding energy of ∼286 eV) from amorphous/graphitic carbon (∼284 eV). Moreover, XPS can also differentiate between the different binding geometries (hollow-bridge vs on-top) of molecular CO on Pd(111) (binding energy difference ca. 0.75 eV) [14] and other surfaces.[37,38] Being element-specific and quantitative, XPS also provides direct information on the amount of the different adsorbates.[39]

* Corresponding author. E-mail: rupprechter@fhi-berlin.mpg.de. Tel: +49 30 8413 4132. Fax: +49 30 8413 4105.

10.1021/jp021992t CCC: $25.00
Published on Web 03/25/2003

Although conventional XPS is limited to low pressures (due to the large mean free path required for photoelectrons to reach the detector), we were able to increase the working pressure up to 0.1 mbar by using a special spectrometer construction. This is at least 5 orders of magnitude higher than conventional XPS and in the range of the high-pressure SFG measurements. It also allows us to establish an equilibrium coverage of CO during measurements at room temperature and above (whereas in UHV part of CO may desorb from the surface at these temperatures, including electron-stimulated desorption during XPS measurements). A further advantage of in situ vs posttreatment measurements is, of course, that there is no possible contamination during pump-down.

The combined application of XPS core-level and SFG vibrational spectroscopy is therefore a further step in an effort to link surface science and technical catalysis. Though SFG allows us to distinguish the different CO adsorptions sites, XPS is particularly suited to examine the chemical nature and quantity of the adsorbed species. Along the same lines, nonlinear optical methods have been used in conjunction with XPS to study, for example, the adsorption, growth, and coverage of self-organizing thiol films on gold.[40]

In this paper, we present core-level XPS and SFG vibrational spectra of carbon monoxide on Pd(111) single-crystal surfaces measured in situ over a wide range of pressures and temperatures (10^{-6} to 1 mbar, 200−400 K) to identify potential high-pressure structures, the nature of adsorbed carbon species, and the possibility of CO dissociation.

Experimental Section

The experiments were carried out in two UHV chambers, located at the Boreskov Institute of Catalysis (XPS) [22,41] and the Fritz-Haber-Institute (SFG).[23,42] Both systems are equipped with high-pressure reaction cells that allow in situ studies. The same Pd(111) single crystal ($1.5 \times 5 \times 10$ mm) was used for the experiments, prepared by standard cutting and polishing techniques. The crystal was mounted between Mo or W wires and could be heated to 1300 K and cooled with liquid nitrogen to 90 K. The Pd(111) surface was cleaned by a sequence of flash annealing to 1250 K, Ar ion etching (beam energy 1−2 keV at 2×10^{-5} mbar Ar at 300 K), heating to 1200 K, oxidation during cooling in 5×10^{-7} mbar O_2 between 1200 and 600 K, and final flash to 1200 K in UHV. After a few cycles, no contaminants were registered by XPS or Auger electron spectroscopy (AES) and the surface was characterized by a sharp (1×1) LEED pattern.[24]

Photoelectron spectroscopy measurements were carried out using a VG ESCALAB "high-pressure" electron spectrometer. Its construction has been described elsewhere.[22,41,43] In short, this setup is equipped with X-ray and UV-photoelectron spectroscopy, LEED, and TPD. The original data acquisition system is used for XPS signal detection and control of the sample temperature.[41] All spectra were taken using nonmonochromatized Al Kα irradiation ($h\nu = 1486.6$ eV) with a constant analyzer pass energy and a resolution of about 1.2 eV. Before measurements, the spectrometer was calibrated using the $Au4f_{7/2}$ binding energy (BE) of 84.00 eV and $Cu2p_{3/2}$ BE of 932.6 eV as references. The takeoff angle between the analyzed photoelectrons and the substrate surface was 70°, with an X-ray incidence angle of 20°. The base pressure of the chamber was about 5×10^{-10} mbar. Differential pumping of the energy analyzer and X-ray tube with diffusion pumps allows us to measure photoemission spectra up to 10^{-4} mbar in the analyzer chamber. By insertion of the special gas cell into the analyzer chamber the pressure could be increased up to 0.1 mbar, but the XPS intensity decreased by 20−30 times.[44] As a consequence, typical XPS collecting times were increased to about 3 h for a high-pressure measurement compared to 30 min in UHV.

Details of the two-level design of the SFG-system were published elsewhere.[23,42] Briefly, samples are prepared and characterized in the upper UHV level (base pressure 1×10^{-10} mbar) equipped with LEED, AES, and TPD. Using an $xyz\varphi$ manipulator, the sample can transferred under UHV to the SFG-compatible reaction cell in the lower level. During this operation the sample holder is inserted into an arrangement of three differentially pumped spring-loaded Teflon seals and the SFG cell is separated from the UHV part. The SFG cell is equipped with two CaF_2 windows to allow infrared and visible light to enter, and to allow sum frequency light to exit to the detector. SFG spectra can be acquired from UHV to atmospheric pressure (with the upper chamber still at 5×10^{-10} mbar) and take about 20 min.

For details about SFG spectroscopy we refer to the literature.[23,45−51] Picosecond laser pulses at a tunable infrared frequency ω_{IR} and at a fixed visible frequency ω_{VIS} are spatially and temporally overlapped on the CO/Pd(111) surface. When the IR frequency is scanned over a vibrational resonance of CO, an SFG signal is generated at the sum frequency ($\omega_{SFG} = \omega_{IR} + \omega_{vis}$). Plotting the SFG intensity vs the IR wavenumber results in a vibrational spectrum. Because SFG is not allowed in media with inversion symmetry, the SFG signal is mainly generated by adsorbed CO, whereas the centrosymmetric Pd bulk and the isotropic gas phase give only a small contribution to the signal. However, when a significant part of the IR light is absorbed in the CO gas phase (>1 mbar) the SFG signal must be normalized to the actual IR and vis intensities at the sample surface.[24,52]

High-purity gases were introduced through variable leak valves. Special attention was paid to the purity of carbon monoxide. In a previous paper,[19] we have stressed that great care has to be taken to control the CO cleanliness during high-pressure experiments. As is well-known, carbon monoxide can easily react with walls of a steel cylinder, containing Ni and Fe, and form volatile Ni and Fe carbonyls. They can decompose on the Pd(111) surface and produce noticeable amounts of graphite or carbonaceous species, and deposited Ni and Fe can also serve to dissociate CO. In the SFG experiments, the impurities were removed by passing CO over a carbonyl absorber cartridge and a cold trap filled with a liquid nitrogen/ethanol mixture (~170 K). No impurities were registered with a differentially pumped mass spectrometer in this case.[19] In the XPS experiments, the whole balloon of CO was cooled with liquid nitrogen. No surface contaminants were registered in high-sensitivity survey XPS spectra even after high-pressure treatments of 5−6 h.

Results and Discussion

The CO/Pd(111) system has been studied by several groups, e.g., those of Bradshaw,[6,7] Hoffmann,[10] Ertl,[3] Somorjai,[5] Goodman,[12] and others,[2] using a large variety of surface-sensitive techniques: TPD,[1,2] LEED,[3−8] XPD,[9] IRAS,[6,7,10−13] XPS,[14] STM,[15,16] etc. Vibrational spectroscopies such as IRAS, electron energy loss spectroscopy (EELS) or SFG allow study of the interaction of CO with well-ordered single-crystal surfaces and in many cases the observed CO stretching frequency can be used to identify specific binding sites (terminal (on-top), 2-fold bridging, and 3- and 4-fold hollow).[53] It should be noted, however, that binding site assignments that are only based on vibrational frequencies may not always be correct.[9]

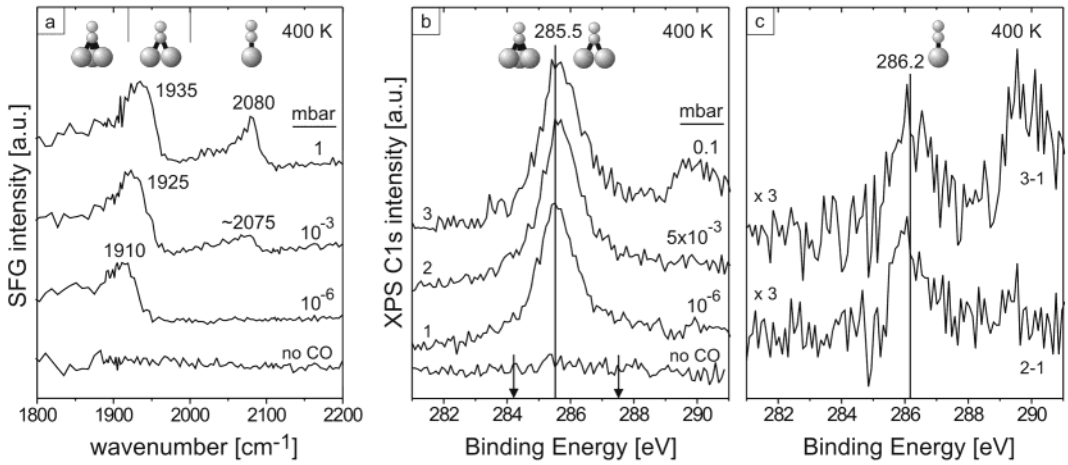

Figure 1. (a) SFG spectra of CO adsorption on Pd(111) at 400 K from 10^{-6} to 1 mbar (approximate frequency ranges of hollow, bridge, and on-top CO are also shown). (b) C1s core-level spectra measured during CO adsorption at 400 K and 10^{-6} mbar (1), 5×10^{-3} mbar (2), and 0.1 mbar (3) and C1s spectrum of the clean surface (no CO). (c) shows the corresponding difference spectra. The arrows indicate C1s binding energies of carbon (~284.2 eV) and carbonyls (~287.5 eV); see text. All XPS spectra were normalized to the Pd3d integral intensity.

These investigations have shown that CO is molecularly bonded to the Pd(111) surface through the carbon atom, with the saturation coverage being temperature-dependent. Thus, the saturation coverage is 0.66 monolayer at $T_{ads} = 200$ K[3] (1 monolayer equals the density of Pd atoms in the (111) plane; 1.53×10^{15} cm^{-2}) and 0.75 monolayer at $T_{ads} = 100$ K.[6] A large number of ordered phases (at least 17) was observed as a function of the CO coverage, which makes CO/Pd(111) a rather complex system. However, all ordered phases have been described in the terms of three adsorption sites: 3-fold hollow, bridge, and on-top, the relative population of which determines the structure of the adlayer. The order of their stability is 3-fold hollow > bridge > on-top. For an isolated CO molecule on Pd(111), the bridge and on-top sites are 0.2 and 0.65 eV higher in energy than the most stable fcc hollow site.[54] However, the relative stability of the three sites is not the only factor that determines the surface structure—it is also influenced by the combination of attractive Pd−CO and repulsive CO−CO interactions. Nevertheless, the development of the different CO adsorbate phases with coverage seems rather well understood.[54]

At low CO coverage, up to 0.33 monolayer, fcc 3-fold hollow sites are populated in the $(\sqrt{3}\times\sqrt{3})$R30° structure. This has been confirmed by STM, XPD, and LEED $I-V$ analysis.[5,8,9,16] IRAS studies have shown the following dependence of the C−O stretching frequency on the CO coverage: at very low coverage, a band appears at 1810−1820 cm^{-1}, which shifts to 1840−1850 cm^{-1}, when the $(\sqrt{3}\times\sqrt{3})$R30° structure is formed. [10] This is in agreement with the calculated anharmonic frequencies of 3-fold hollow sites: 1828−1830 cm^{-1} at 0.33 monolayer.[54]

At 0.5 monolayer a peak at 1925 cm^{-1} was observed and, according to photoemission, photoelectron diffraction, and stretching frequency calculations, assigned to CO in fcc and hcp 3-fold hollow sites.[9,14,54] Total energy calculations by Loffreda and Sautet[54] reveal that these two sites are most favorable with only a small energy difference (0.03 eV) between the fcc and the hcp sites. In a recent STM study Rose et al.[16] were able to resolve both CO molecules within the c(4×2) unit cell and could show that near $\theta = 0.5$ actually two types of c(4×2) structures coexisted. One with CO in fcc and hcp 3-fold hollow sites and one with bridge bonded c(4×2) (as originally suggested by vibrational spectroscopy).[10]

Between 0.5 and 0.6 monolayer, the structure consists of a mixture of phase and antiphase domains with a local CO density of 0.5 monolayer and the $(\sqrt{3}\times2)$rect structure.[6,13] Above $\theta =$ 0.6, CO is preferentially bridge bonded (1950 cm^{-1}) with a smaller amount of linear (on-top) CO at ~2090 cm^{-1}.[6,7] At even higher coverages, the adsorbate rearranges and 3-fold hollow and on-top sites are populated. Finally, at saturation coverage ($\theta = 0.75$) two bands at 1895 and 2106 cm^{-1} (fcc and hcp hollow and on-top CO) were observed, producing a (2×2) structure.[6,12,16] Well-defined structures occur at 0.5 monolayer [c(4×2) or $(\sqrt{3}\times2)$rect] and at 0.6 monolayer [c$(\sqrt{3}\times5)$rect].[6]

With respect to our study, the high-resolution XPS data of Surnev et al.[14] are particularly interesting. These authors have studied CO adsorption on Pd(111) under UHV conditions using synchrotron radiation. By analyzing the coverage-dependent sequence of CO phases obtained at 100 K, the C1s feature at 285.6 ± 0.1 eV was assigned to CO adsorbed in 3-fold hollow sites, a feature at 285.85 to bridge-bonded CO, and a feature at 286.3 eV to on-top CO.

Figure 1 shows SFG and XPS spectra acquired at 400 K for CO pressures up to 1 mbar. For the clean surface both SFG and XPS showed a flat baseline, indicating that CO adsorption from the residual gas was negligible (all XPS spectra were normalized to the Pd3d integral intensity at 335.4 eV). At 10^{-6} mbar CO, on the basis of the various studies mentioned above, SFG indicated that CO was bonded on hollow sites with a coverage below 0.5 monolayer (Figure 1a), with the strong coverage dependence of the CO stretching frequency being a good indication for the CO structure and coverage.[19] However, considering the STM results by Rose et al. [16] the presence of bridge-bonded CO cannot be fully excluded.

Under the same conditions, the corresponding C1s core-level spectrum in Figure 1b showed only a narrow peak at 285.5 eV with a fwhm (full width at half maximum) of about 1.3 eV. According to high-resolution XPS,[14] this C1s feature can be assigned to CO in 3-fold hollow sites. It should, however, be noted that due to the limited resolution of our XPS system, 3-fold hollow and bridge-bonded CO cannot be differentiated. Nevertheless, the C1s peak position and its small fwhm suggest that CO preferentially adsorbed at the more stable 3-fold hollow and bridge sites whereas on-top CO was absent, in agreement with SFG (Figure 1a).

Increasing the pressure to 10^{-3} mbar shifted the CO frequency to 1925 cm^{-1} and produced a weak on-top signal at ~2075 cm^{-1}. This indicated that the coverage was around 0.5 monolayer. At 5×10^{-3} mbar the XPS spectrum displayed, apart from the 285.5 eV peak, a shoulder at the high-BE side, which

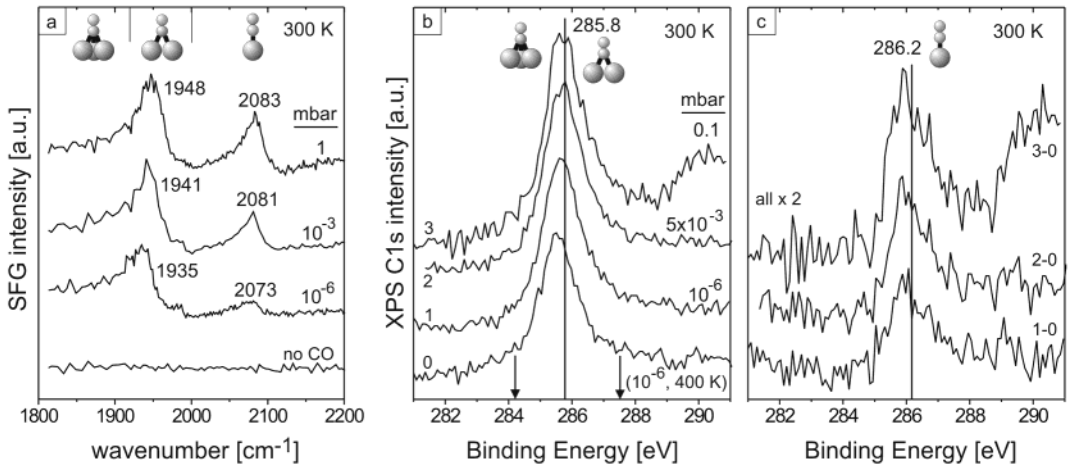

Figure 2. (a) SFG spectra of CO adsorption on Pd(111) at 300 K from 10^{-6} to 1 mbar. (b) C1s core-level spectra measured during CO adsorption at 300 K and 10^{-6} mbar (1), 5×10^{-3} mbar (2), and 0.1 mbar (3) and at 400 K and 10^{-6} mbar (0). (c) shows the corresponding difference spectra. All XPS spectra were normalized to the Pd3d integral intensity.

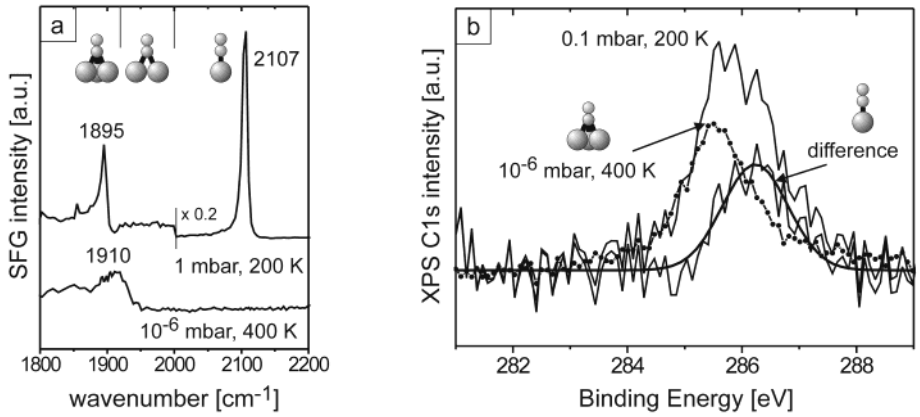

Figure 3. (a) SFG spectra of CO adsorption on Pd(111) at 1 mbar/200 K and 10^{-6} mbar/400 K. (b) C1s core-level spectra at 0.1 mbar/200 K and 10^{-6} mbar/400 K. The difference spectrum represents the contribution of on-top bonded CO (see text). All XPS spectra were normalized to the Pd3d integral intensity.

was due to the presence of another component. By subtracting the 10^{-6} mbar from the 5×10^{-3} mbar C1s spectrum in Figure 1c, one can identify a new peak at 286.2 eV due to CO adsorption on on-top sites.[14] At 1 mbar CO, SFG indicated the presence of bridge and on-top CO, in agreement with the XPS spectra at 0.1 mbar. The C1s feature at ~290 eV originates from gas phase CO and typically occurred above 10^{-2} mbar.

It should be noted that both SFG and XPS only indicated the presence of "regular" CO adsorption species (hollow, bridge, on-top). No signatures of high-pressure species were found. Palladium carbonyl species would produce a C1s XPS signal at 287−288 eV.[55] This range is not obscured by adsorbed or gas-phase CO; therefore we can exclude the presence of carbonyls. The dissociation of CO by the Boudouard reaction (or the decomposition of Pd carbonyls) would lead to carbon deposition[29,30] and should produce a feature at 284.0 eV characteristic of graphite or at 284.4 eV from amorphous carbon. In the case of carbide species a feature at lower binding energy (<283.5 eV) would appear. Even if carbon dissolved in the Pd bulk near the surface region, the escape depth of the C1s electrons (about 2 nm) should have been sufficient to allow its detection. The absence of any carbon related signals indicates that CO does not dissociate at 400 K and ~1 mbar, even over several hours. SFG spectra acquired up to 1000 mbar also did not show any indication of CO dissociation.[19,24]

Increasing the CO pressure from 10^{-6} to 1 mbar at 400 K increased the amount of on-top bonded CO (Figure 1). A similar effect was, of course, observed upon decreasing the temperature. Figure 2 shows analogous SFG and XPS measurements at 300 K. At 10^{-6} mbar, SFG indicated bridge and on-top bonded CO (Figure 2a). Increasing the CO pressure led to frequency shifts due to dipole coupling and to an increase in the on-top intensity. The growing on-top population was also evident from the corresponding XPS spectra in Figure 2b,c. Because on-top CO was present at 300 K at all pressures studied (Figure 2a), the difference spectra in Figure 2c used the 10^{-6} mbar/400 K C1s spectrum for subtraction.

Measurements at 200 K followed the same trends (with, of course, higher coverages at the respective pressures).[24] Figure 3a shows the 1 mbar SFG spectrum at 200 K, when a perfect 0.75 monolayer (2×2) structure with CO in hollow and on-top sites was produced.[6,12] The corresponding 0.1 mbar XPS measurement is presented in Figure 3b, but the absence of clear shoulders in the C1s spectrum of adsorbed CO made it impossible to directly deconvolute this spectrum into hollow and on-top components. Therefore, to estimate the ratio between hollow and on-top population, we subtracted the C1s spectrum measured at 10^{-6} mbar and 400 K (when SFG indicated ~0.5 monolayer hollow bonded CO, with on-top CO being absent) from the spectrum measured at 0.1 mbar and 200 K (when SFG indicated the coexistence of 3-fold hollow and on-top CO, Figure 3a). The difference spectrum clearly reveals the on-top contribution. Integration of these spectra and calculating the intensity ratio of the 3-fold hollow C1s spectrum (10^{-6} mbar/400 K) to

TABLE 1: Quantitative Analysis of XPS and SFG Data[a]

XPS				SFG			
θ, monolayer	200 K	300 K	400 K	θ, monolayer	200 K	300 K	400 K
1×10^{-6} mbar	0.63	0.50	0.38	1×10^{-6} mbar	0.65	0.5	0.45
5×10^{-3} mbar	0.71	0.53	0.46	1×10^{-3} mbar	0.7	0.55	0.5
1×10^{-1} mbar	0.71	0.63	0.48	1 mbar		0.75	0.6	0.55

[a] For XPS, the 0.63 monolayer structure formed at 1×10^{-6} mbar/200 K was used as the reference. In the case of SFG, the coverage was estimated (±0.05 monolayer) on the basis of the strong coverage dependence of the C−O stretching frequency, using spectra of well ordered structures at 0.5, 0.63 and 0.75 monolayer as references.[24]

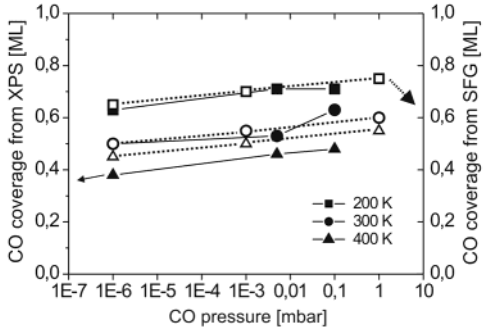

Figure 4. Coverage vs pressure dependence determined from XPS (full symbols, full lines) and from SFG (open symbols, dashed lines). See also Table 1.

the difference/on-top spectrum yielded a hollow/on-top ratio of 1.8. This is in reasonable agreement with a hollow/on-top ratio of 2 arising from the (2×2) CO structure proposed for the saturation coverage.[6]

The CO coverage as a function of pressure, as determined from XPS, is shown for the different temperatures in Table 1. The CO structure at 10^{-6} mbar and 200 K ($\theta = 0.63$ monolayer), i.e., the total area of the corresponding C1s spectrum, was used as the reference point. CO coverages estimated from the CO stretching frequency in the SFG spectra are also given in Table 1 and are in good agreement with XPS. Both methods show that already at 200 K a pressure of 0.1−1 mbar is necessary to reach the CO saturation coverage of $\theta = 0.75$ monolayer. Under typically UHV pressures this structure is only obtained around 100 K.[6] The coverage/pressure relationship is graphically shown in Figure 4.

Summarizing, we did not observe CO dissociation on Pd(111) under our experimental conditions. However, several groups observed partial CO dissociation on Pd nanoparticles supported on different supports. Doering et al.[31] studied 2−7.5 nm Pd particles on mica and reported a higher CO dissociation rate for smaller particle sizes and a preferred blocking of strongly bonding adsorption sites by residual carbon. Matolin et al.[32−35] observed CO dissociation on 2−3 nm Pd particles on MgO and alumina. Rainer et al.[36] observed CO dissociation on similar particles above 400 K and 10^{-5} mbar CO. These results suggest that CO dissociation requires low-coordinated (defect) sites that are only present on Pd nanoparticles or on rough surfaces.[23,28,31,56] This picture is further supported by the observation of Matolin and co-workers that CO dissociation occurred on sputtered, defect-rich Pd foil but was absent on the annealed foil.[33] Considering that CO is stronger bonded on defect sites, the concomitant weakening of the C−O bond may be (partly) responsible for CO dissociation (neglecting any support effects).[35] In fact, SFG spectra of CO on strongly sputtered Pd(111) surfaces have shown an additional feature at ~1990 cm^{-1}, which was assigned to defect (step) sites.[19,24] These sites may be the centers for CO dissociation. High-pressure XPS spectra of CO on stepped Pd surfaces and supported nanoparticles will be measured in the future.

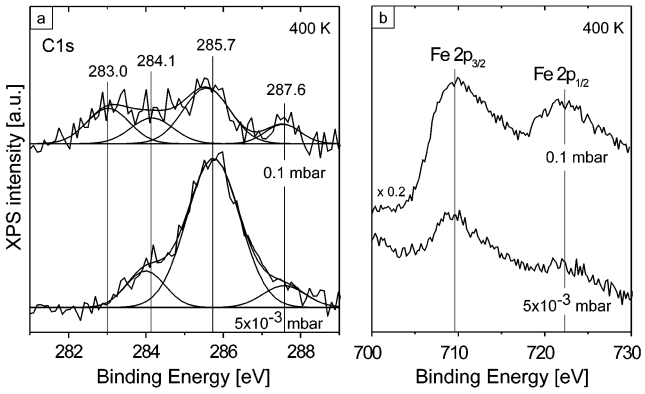

Figure 5. (a) C1s and (b) Fe2p core-level spectra obtained when CO was used without purification at 400 K, at 5×10^{-3} mbar and 0.1 mbar. Results of deconvoluting the C1s spectra are also shown in (a): 283.0, carbide species (FeC); 284.1, graphite; 285.7, molecular CO; 287.6, carbonyl species.

Finally, we want to stress that special attention must be paid to CO cleanliness.[19] Figure 5 shows C1s and Fe2p spectra measured during CO adsorption at 400 K and different pressures when research grade 4.7 CO was used without further purification. One can see that in addition to the C1s signal from molecular CO (~285.7 eV) two other features at 284.1 and 287.6 eV were observed. As already mentioned above, these signals can be assigned to graphitic/amorphous carbon and to carbonyls, respectively. This indicates that if the gas was not properly cleaned from $Fe(CO)_5$ and $Ni(CO)_4$, the decomposition of these compounds and a possible CO dissociation on deposited Ni or Fe can easily produce additional C1s signals. Iron carbonyl was the reason in the present case, as evident from the appearance of Fe2p signals (Figure 5b), whereas a possible Ni contamination has been reported in ref 19. At higher CO pressure, even stronger Fe signals were observed, leading to a decrease of molecular CO and to the appearance of an additional C1s signal originating from iron carbides (283.0 eV). Apparently, great care has to be taken not to misinterpret such observations as being due to CO dissociation on Pd.

Conclusions

CO adsorption on Pd(111) was examined by high-pressure SFG and XPS from 200 to 400 K, and between 10^{-6} and 1 mbar CO. Even under high pressure both methods indicated that CO adsorbed in "regular" adsorption sites such as hollow, bridge, and on-top. The high-pressure CO structures were similar to those known from UHV studies. Our data clearly demonstrate that, by combination of SFG and XPS, adsorbate structures and coverages can be obtained in situ at high pressure and they even allow a quantitative analysis. In comparison to typical UHV studies, we were able to extend the pressure range by at least 5 orders of magnitude.

We did not observe any indications of CO dissociation or carbonyl formation under our experimental conditions. In light of previous studies on Pd(111) and Pd nanoparticles it seems that CO dissociation requires the presence of low-coordination (defect) sites. Consequently, analogous experiments on sputtered and stepped Pd surfaces and supported Pd nanoparticles are planned for the near future.

Acknowledgment. Part of this work was supported by the German Science Foundation (DFG) through priority program SPP1091.

References and Notes

(1) Noordermeer, A.; Kok, G. A.; Nieuwenhuys, B. E. *Surf. Sci.* **1986**, *172*, 349.
(2) Guo, X.; Yates, J. T. *J. Chem. Phys.* **1989**, *90*, 6761.
(3) Conrad, H.; Ertl, G.; Küppers, J. *Surf. Sci.* **1978**, *76*, 323.
(4) Biberian, J. P.; Van Hove, M. A. *Surf. Sci.* **1984**, *138*, 361.
(5) Ohtani, H.; Van Hove, M. A.; Somorjai, G. A. *Surf. Sci.* **1987**, *187*, 372.
(6) Tüshaus, M.; Berndt, W.; Conrad, H.; Bradshaw, A. M.; Persson, B. *Appl. Phys. A* **1990**, *51*, 91.
(7) Bradshaw, A. M.; Hoffmann, F. M. *Surf. Sci.* **1978**, *72*, 513.
(8) Zasada, I.; Van Hove, M. A. *Surf. Sci.* **2000**, *457*, L421.
(9) Giessel, T.; Schaff, O.; Hirschmugl, C. J.; Fernandez, V.; Schindler, K. M.; Theobald, A.; Bao, S.; Lindsay, R.; Berndt, W.; Bradshaw, A. M.; Baddeley, C.; Lee, A. F.; Lambert, R. M.; Woodruff, D. P. *Surf. Sci.* **1998**, *406*, 90.
(10) Hoffmann, F. M. *Surf. Sci. Rep.* **1983**, *3*, 103.
(11) Gelin, P.; Siedle, A.; Yates, J. *J. Phys. Chem.* **1984**, *88*, 2978.
(12) Kuhn, W. K.; Szanyi, J.; Goodman, D. W. *Surf. Sci. Lett.* **1992**, *274*, L611.
(13) Bourguignon, B.; Carrez, S.; Dragnea, B.; Dubost, H. *Surf. Sci.* **1998**, *418*, 171.
(14) Surnev, S.; Sock, M.; Ramsey, M. G.; Netzer, F. P.; M.Wiklund; Borg, M.; Andersen, J. N. *Surf. Sci.* **2000**, *470*, 171.
(15) Sautet, P.; Rose, M. K.; Dunphy, J. C.; Behler, S.; Salmeron, M. *Surf. Sci.* **2000**, *453*, 25.
(16) Rose, M. K.; Mitsui, T.; Dunphy, J.; Borg, A.; Ogletree, D. F.; Salmeron, M.; Sautet, P. *Surf. Sci.* **2002**, *512*, 48.
(17) Somorjai, G. A.; Rupprechter, G. *J. Phys. Chem. B* **1999**, *103*, 1623.
(18) Dellwig, T.; Rupprechter, G.; Unterhalt, H.; Freund, H.-J. *Phys. Rev. Lett.* **2000**, *85*, 776.
(19) Rupprechter, G.; Unterhalt, H.; Morkel, M.; Galletto, P.; Hu, L.; Freund, H.-J. *Surf. Sci.* **2002**, *502*−*503*, 109.
(20) Freund, H.-J.; Ernst, N.; Risse, T.; Hamann, H.; Rupprechter, G. *Phys. Status Solidi A* **2001**, *187*, 257.
(21) Knop-Gericke, A.; Hävecker, M.; Schedel-Niedrig, T.; Schlögl, R. *Top. Catal.* **2001**, *15*, 27.
(22) Bukhtiyarov, V. I.; Kaichev, V. V.; Podgornov, E. A.; Prosvirin, I. P. *Catal. Lett.* **1999**, *57*, 233.
(23) Rupprechter, G. *Phys. Chem. Chem. Phys.* **2001**, *3*, 4621.
(24) Unterhalt, H.; Rupprechter, G.; Freund, H.-J. *J. Phys. Chem. B* **2002**, *106*, 356.
(25) Conrad, H.; Ertl, G.; Koch, J.; Latta, E. E. *Surf. Sci.* **1974**, *43*, 462.
(26) Weissman, D. L.; Shek, M. L.; Spicer, W. E. *Surf. Sci.* **1980**, *92*, L59.
(27) Broden, G.; Rhodin, T. N.; Bruckner, C. F.; Benbow, R.; Hurych, Z. *Surf. Sci.* **1976**, *59*, 593.
(28) Stara, I.; Matolin, V. *Surf. Sci.* **1994**, *313*, 99.
(29) Kung, K. Y.; Chen, P.; Wei, F.; Shen, Y. R.; Somorjai, G. A. *Surf. Sci. Lett.* **2000**, *463*, L627.
(30) McCrea, K.; Parker, J. S.; Chen, P.; Somorjai, G. A. *Surf. Sci.* **2001**, *494*, 238.
(31) Doering, D. L.; Poppa, H.; Dickinson, J. T. *J. Catal.* **1982**, *73*, 104.
(32) Matolin, V.; Gillet, E. *Surf. Sci.* **1990**, *238*, 75.
(33) Matolin, V.; Rebholz, M.; Kruse, N. *Surf. Sci.* **1991**, *245*, 233.
(34) Johánek, V.; Stará, I.; Tsud, N.; Veltruská, K.; Matolín, V. *Appl. Surf. Sci.* **2000**, *162*−*163*, 679.
(35) Tsud, N.; Johánek, V.; Stará, I.; Veltruská, K.; Matolín, V. *Surf. Sci.* **2000**, *467*, 169.
(36) Rainer, D. R.; Xu, C.; Holmblad, P. M.; Goodman, D. W. *J. Vac. Sci. Technol. A* **1997**, *15*, 1653.
(37) Broden, G.; Pirug, G.; Bonzel, H. *Chem. Phys. Lett.* **1977**, *51*, 250.
(38) Held, G.; Schuler, J.; Sklarek, W.; Steinrück, H.-P. *Surf. Sci.* **1998**, *398*, 154.
(39) Au, C. T.; Carley, A. F.; Roberts, M. W. *Int. Rev. Phys. Chem.* **1986**, *5*, 57.
(40) Buck, M.; Eisert, F.; Fischer, J.; Grunze, M.; Träger, F. *Appl. Phys. A* **1991**, *53*, 552.
(41) Kaichev, V. V.; Sorokin, A. M.; Timoshin, A. I.; Vovk, E. I. *Instrum. Exp. Techniques* **2002**, *45*, 50.
(42) Rupprechter, G.; Dellwig, T.; Unterhalt, H.; Freund, H.-J. *Top. Catal.* **2001**, *15*, 19.
(43) Joyner, R. W.; Roberts, M. W.; Yates, K. *Surf. Sci.* **1979**, *87*, 501.
(44) Bukhtiyarov, V. I.; Prosvirin, I. P. *Proc. Eur. Congr. Catal.* **2001**, 21.
(45) Shen, Y. R. *Nature* **1989**, *337*, 519.
(46) Bandara, A.; Dobashi, S.; Kubota, J.; Onda, K.; Wada, A.; Domen, K.; Hirose, C.; Kano, S. *Surf. Sci.* **1997**, *387*, 312.
(47) Tadjeddine, A.; Le Rille, A.; Pluchery, O.; Vidal, F.; Zheng, W. Q.; Peremans, A. *Phys. Status Solidi A* **1999**, *175*, 89.
(48) Braun, R.; Casson, B. D.; Bain, C. D.; van der Ham, E. W. M.; Vrehen, Q. H. F.; Eliel, E. R.; Briggs, A. M.; Davies, P. B. *J. Chem. Phys.* **1999**, *110*, 4634.
(49) Lin, S.; Oldfield, A.; Klenerman, D. *Surf. Sci.* **2000**, *464*, 1.
(50) Williams, C. T.; Yang, Y.; Bain, C. D. *Catal. Lett.* **1999**, *61*, 7.
(51) Härle, H.; Lehnert, A.; Metka, U.; Volpp, H. R.; Willms, L.; Wolfrum, J. *Chem. Phys. Lett.* **1998**, *293*, 26.
(52) Rupprechter, G.; Dellwig, T.; Unterhalt, H.; Freund, H.-J. *J. Phys. Chem. B* **2001**, *105*, 3797.
(53) Sheppard, N.; Nguyen, T. T. *Adv. Infrared Raman Spectrosc.* **1978**, *5*, 67.
(54) Loffreda, D.; Simon, D.; Sautet, P. *Surf. Sci.* **1999**, *425*, 68.
(55) Barber, M.; Connor, J. A.; Guest, M. F.; Hall, M. B.; Hillier, I. H.; Meredith, W. N. E. *Faraday Discuss. Chem. Soc.* **1972**, *54*, 219.
(56) Rupprechter, G.; Freund, H.-J. *Top. Catal.* **2001**, *14*, 3.